ROBUST AND MODERN CONTROL OF VSC-HVDC

Affane GHALEM[1], Allaoui TAYEB[2], Smaili ATTALLAH[3] , Kouadria Mohamed ABDELDJABBAR[4]

This paper contains a set of controls on the VSC-HVDC system aimed at selecting the best control capable of making the system withstands the impact of internal and external interference from nearby devices and make it more suitable in complex electrical networks. Among these controls is control by conventional PID, IMC control. The validity of these controls applied to the VSC-HVDC system has been investigated by MATLB/Simulink. Sealing this work by comparing and choosing the best control makes the system more stable and the demand of industrial and commercial electrical partners.

Keywords: VSC-HVDC, PID, IMC.

1. Introduction

To Today we find the technological and commercial competition in the field of renewable energy in a very rapid and terrible development, and that the most important of which is to eliminate the pollution problem that is currently taking place in the world and the interconnection between countries. Wind energy is one of the most promising renewable sources of energy for the preservation of the environment. The development of these energies was mainly based on power electronic and the automatically control. The Voltage Source Converter based High Voltage Direct Current (VSC-HVDC) installation has several advantages compared to conventional High voltage Direct Voltage (HVDC) such as, independent control of active and reactive power, reversal of power without changing the polarity of dc voltage and no requirement of fast communication between the two converter stations [1],[2]. The (VSC-HVDC) lines are seen as the preferred solution for accommodation the increase in renewable energies and additional interconnection capacity due to their controllability and adequacy for long underground and undersea connections [3].In order to make the

[1] Department of Electrical Engineering, Laboratory of Energetic and Computer Engineering, IbnKhaldun University, Tiaret 14000, Algeria, e-mail: g_affene@yahoo.fr
[2] Department of Electrical Engineering, Laboratory of Energetic and Computer Engineering, IbnKhaldun University, Tiaret 14000, Algeria, e-mail: allaoui_tb@yahoo.fr
[3] Department of Electrical Engineering, Laboratory of Energetic and Computer Engineering, IbnKhaldun University, Tiaret 14000, Algeria, e-mail: smaili_at@yahoo.fr
[4] Department of Electrical Engineering, Laboratory of Energetic and Computer Engineering, IbnKhaldun University, Tiaret 14000, Algeria, e-mail: abdeldjabbar14@yahoo.fr

system(VSC-HVDC) more stable against the internal and external perturbations issued by the surrounding devices must choose the best control suitable for this.

The paper is organized as follows. The configuration of VSC based HVDC link is described in section 1, the modelling of VSC-HVDC system in section 2, control by Proportional-Integral PI and simulation results in section 3, control by IMC discussed in section 4, and 5. Finally; the section 6 presents the conclusions.

2. Configuration of VSC-HVDC System

The figure.1 shows the configuration of VSC based HVDC link, consisting of two different sources AC of frequency, two transformators, two AC filters reactors and DC cable and two converters rectifier and inverter. The VSC as shown in figure.2 are consisted of six-pulse Bridge equipped with self-commutating switches (IGBTs) and diode connected in anti-parallel.

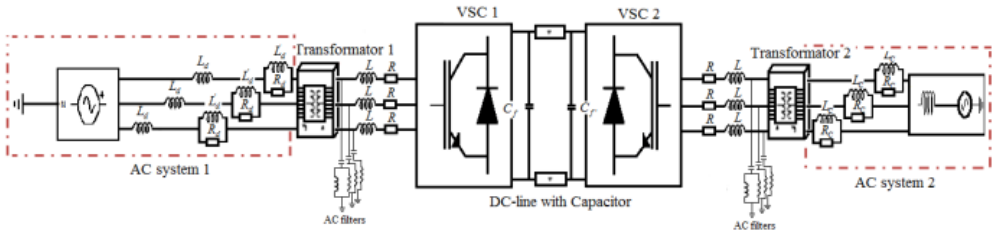

Fig.1. The configuration of VSC based HVDC transmission system

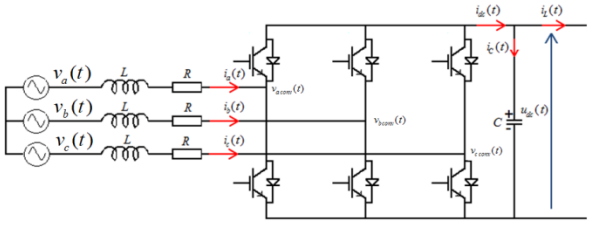

Fig. 2. The structure of VSC-HVDC converter

3. The Modeling of VSC-HVDC system

The mathematic model of VSC-HVDC in three phases:

$$\begin{cases} v_a(s) = L\frac{di_a(t)}{dt} + Ri_a(t) + v_{a\_conv}(t) \\ v_b(s) = L\frac{di_b(t)}{dt} + Ri_b(t) + v_{b\_conv}(t) \\ v_c(s) = L\frac{di_c(t)}{dt} + Ri_c(t) + v_{c\_conv}(t) \\ i_{dc}(t) = C\frac{du_{dc}(t)}{dt} + i_L \end{cases} \quad (1)$$

Where $v_a(s)$, $v_b(s)$ and $v_c(s)$ are component of the AC voltage of transmission network, $i_a(t)$, $i_b(t)$ and $i_c(t)$ are phase currents. L represents the inductance of the phase reactor and R represents the resistance of the phase reactor. $v_{a\_conv}(t)$,$v_{b\_conv}(t)$ and $v_{c\_conv}(t)$ are phases voltage at the side of the converter can be represented by:

$$\begin{cases} v_{a\_conv}(t) = \frac{1}{3}(+2S_a - S_b - S_c)u_{dc}(t) \\ v_{b\_conv}(t) = \frac{1}{3}(-S_a + 2S_b - S_c)u_{dc}(t) \\ v_{c\_conv}(t) = \frac{1}{3}(-S_a - S_b + 2S_c)u_{dc}(t) \\ i_{dc} = \frac{1}{2}[S_a i_a(t) + S_b i_b(t) + S_c i_c(t)] \end{cases} \quad (2)$$

With S_i the switching function defined by $S_i = 1$ upper switch ON, $S_i = 0$ botton switch OFF with phase i=a, b, c. Where $u_{dc}(t)$ and i_{dc} are DC output voltage and current respectively [4],[5].

The dq frame transformation of equation (1), the dq components of the voltage become:

$$\begin{cases} v_d(t) = L\frac{di_d(t)}{dt} + Ri_d(t) - \omega Li_q(t) + v_{d\_conv}(t) \\ v_q(t) = L\frac{di_q(t)}{dt} + Ri_q(t) + \omega Li_d(t) + v_{q\_conv}(t) \end{cases} \quad (3)$$

The equations of the active and reactive power in the dq frame as:

$$\begin{cases} P_{ac} = \frac{3}{2}(v_d i_d + v_q i_q) \\ Q_{ac} = \frac{3}{2}(v_q i_d - v_d i_q) \end{cases} \quad (4)$$

Whit $v_q = 0$ thus the active and reactive power are represented as [6]:

$$\begin{cases} P_{ac} = +\frac{3}{2}v_d i_d \\ Q_{ac} = -\frac{3}{2}v_d i_q \end{cases} \quad (5)$$

The active power balanced relationship between the AC input and DC output are given as [6]:

$$P_{ac} = P_{dc} \Leftrightarrow \frac{3}{2} v_d . i_d = u_{dc} . i_{dc} \tag{6}$$

4. Inner Control Loop

The using equation (3) for the inner controller loop, the current controller block uses the Proportional-Integral PI controller with the transfer function given by

$$C(s) = k_p + \frac{k_i}{S} \tag{7}$$

We propose

$$\begin{cases} v_{d\_reg}(t) = L\frac{di_d(t)}{dt} + Ri_d(t) \\ v_{q\_reg}(t) = L\frac{di_q(t)}{dt} + Ri_q(t) \end{cases} \tag{8}$$

Where $v_{d\_reg}(t)$ and $v_{q\_reg}(t)$ regulate the dq-axis current.

$$\begin{cases} V_{d\_reg}(S) = \left[I_{d\_ref}(S) - I_d(S)\right]\left(k_p + \frac{k_i}{S}\right)\left(\frac{1}{1+T_a S}\right) \\ V_{q\_reg}(S) = \left[I_{q\_ref}(S) - I_q(S)\right]\left(k_p + \frac{k_i}{S}\right)\left(\frac{1}{1+T_a S}\right) \end{cases} \tag{9}$$

Where k_p and k_i are the proportional and integral gains of PI controller are calculating as:

$$\begin{cases} k_p = \frac{L}{4T_a\xi^2} \\ k_i = \frac{R}{4T_a\xi^2} \end{cases} \tag{10}$$

With $T_a = \frac{1}{F_{PWM}}$, where F_{PWM} the switching frequency of the converter block.

The principal of inner control is based from the equation (3). The type of the control allows through a reference current $i_d(t)$ and $i_q(t)$ of the generated reference voltage $v_{cd}(t)$ and $v_{cq}(t)$ for generating control pulses for VSC converter. The detailed block diagram of the complete system is shown as:

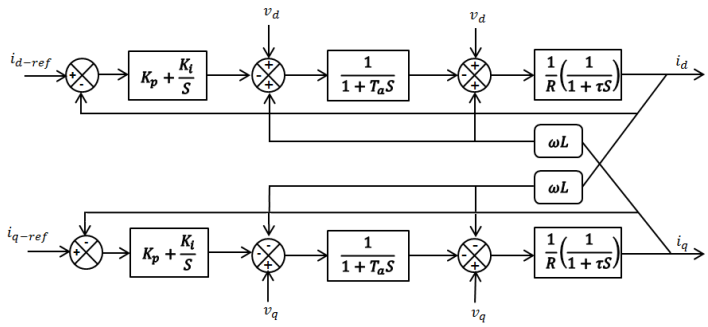

Fig. 3. Detail block diagram of inner controller system

5. Active and Reactive Power Controllers

From the equation (5), the reference current $i_d^*(t)$ and $i_q^*(t)$ becomes:

$$\begin{cases} i_d^*(t) = +\frac{2}{3}\frac{P_{ac}^*(t)}{v_d(t)} \\ i_q^*(t) = -\frac{2}{3}\frac{Q_{ac}^*(t)}{v_d(t)} \end{cases} \quad (11)$$

Where $\mathbf{P_{ac}^*(t)}$ and $Q_{ac}^*(t)$ represent reference active and reactive power. The active and reactive power controller blocks use the Proportional-Integral PI controller. The parameters of PI controller are calculated as:

$$\begin{cases} k_p = \frac{2n}{3v_d} \\ k_i = \frac{n}{3T_a v_d} \end{cases} \quad (12)$$

Where n is natural number

The block diagrams of active and reactive controls are shown on the following fig. (4) and fig. (5):

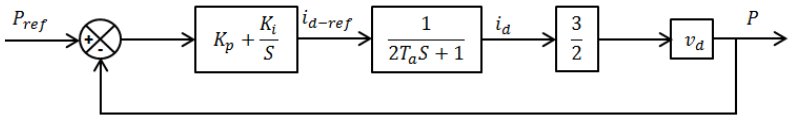

Fig. 4. Block diagram of active power control

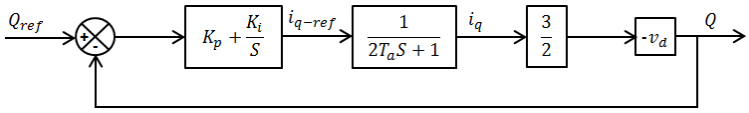

Fig. 5. block diagram of reactive control

6. DC-link model and linearization

The dc-link voltage is modeled as a pure capacitor. This capacitor is energy storage where the stored electrical energy is Joule as [8] :

$$E_c = \frac{1}{2} C . v_{dc}^2(t) \tag{13}$$

With

$$P_c = \frac{1}{2} C \frac{v_{dc}^2(t)}{dt} \tag{14}$$

And

$$P_c = P_{ac}(t) - P_{load}(t) \tag{15}$$

7. Linearization

We now choose a new state variable $h(t) = v_{dc}^2(t)$, the equation (16) becomes:

$$\frac{1}{2} C \frac{dh(t)}{dt} = \frac{3}{2} v_d(t) i_d(t) - \frac{1}{R_{load}} h(t) \tag{16}$$

The choice of regulator which corresponds with this loop is regulator PI classic, after calculations the parameters of regulator are calculated as follow [7]:

$$\begin{cases} k_{p\_dc} = \frac{2n}{3R_{load}} \\ k_{i\_dc} = \frac{4n}{3R_{load}^2 C} \end{cases} \tag{17}$$

The following diagram represents the DC link voltage

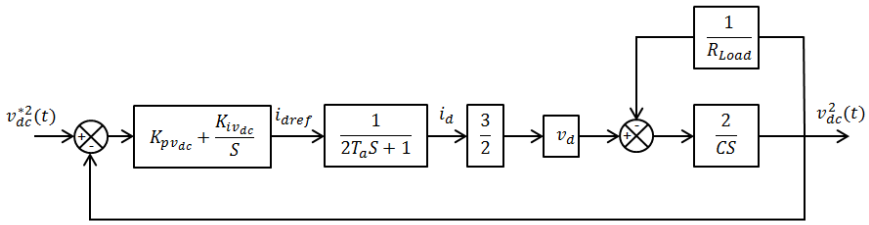

Fig. 6. Block diagram of the DC link voltage controller

8. Simulation Results

After steady state has been reached, a 1.5 pu step is applied to the reference active power at (t=0.2 s) and later a -0.2 pu step is applied to the reference active power at (t=1.0 s). a -0.1 pu step is applied to reference reactive power at (t=0.5s). The dynamic response of the regulators is observed. Stabilizing time is approximately 0.24 s.

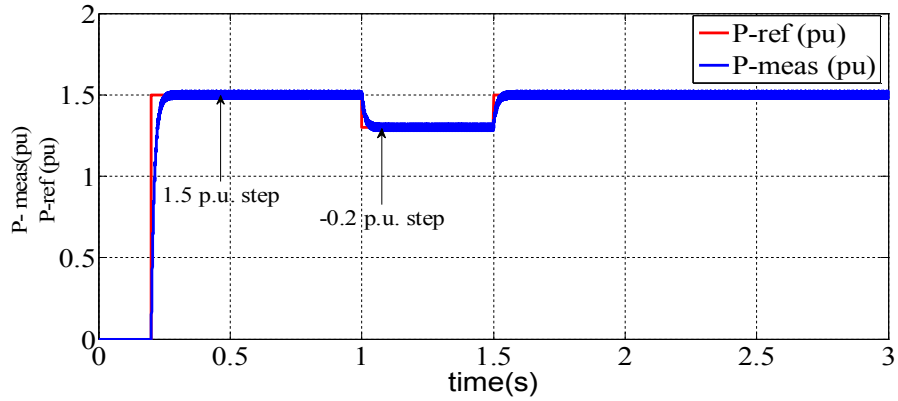

Fig.7 Active Power (pu)

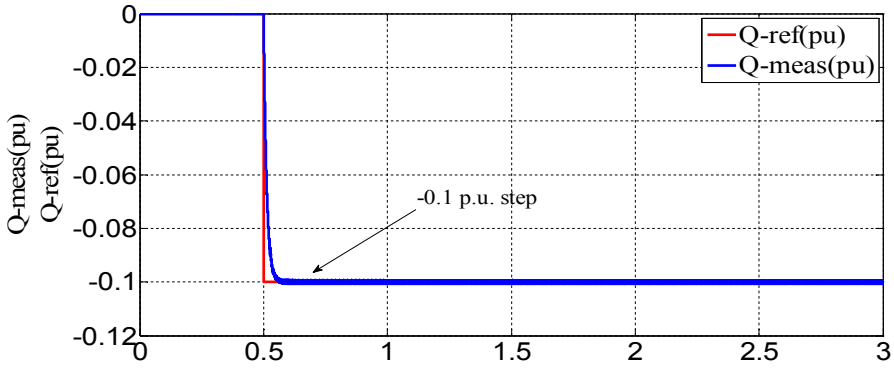

Fig.8. Reactive Pouwer (pu)

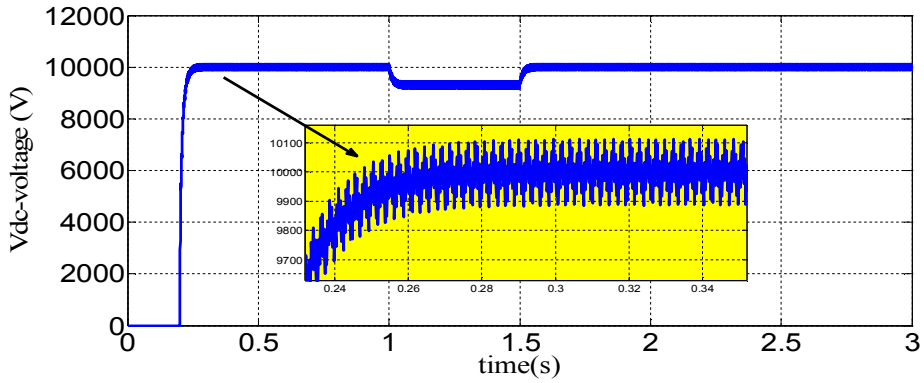

Fig. 9 simulation of Vdc-voltage (V)

9.Internal Model Control (IMC)

Consider the system shown in figure (10), $G_p(s)$ is the plant $\tilde{G}_p(s)$ is the nominal model, R(s) is the desired value, U(s) is the control, d(s) is a disturbance input.

$G_c(s)$ is called the IMC controller and is to be designed so that y(t) is kept as close possible to r(t) at all times.

The feedback signal

$$\tilde{d}(s) = [G_p(s) - \tilde{G}_p(s)]U(s) + d(s) \quad (18)$$

If in equation (19) the model is exact, $G_p(s) = \tilde{G}_p(s)$ and the disturbance d(s) is zero, then $\tilde{d}(s)$ is also zero and the control is effectively open-loop. This is the condition when there is no uncertainty. However, if $G_p(s) = \tilde{G}_p(s)$ and d(s) is not zero, the $\tilde{d}(s)$ expresses the uncertainty of the process.

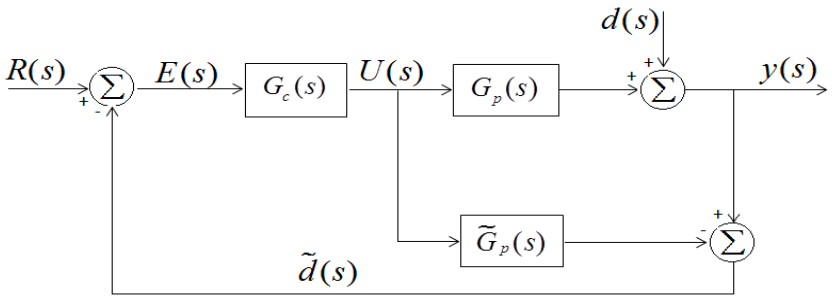

Fig.10. Block diagram of an IMC system

From figure (10) the resulting control signal is given by

$$\begin{cases} U(s) = \left[R(s) - \tilde{d}(s)\right]G_c(s) \\ d(s) = \left[G_p(s) - \tilde{G}_p(s)\right]U(s) + d(s) \\ U(s) = \left[R(s) - \left(G_p(s) - \tilde{G}_p(s)\right)U(s) + d(s)\right]G_c(s) \end{cases} \quad (19)$$

The closed loop transfer function for the IMC scheme is therefore

$$Y(s) = \frac{G_c(s)G_p(s)R(s) + \left[1 - G_c(s)\tilde{G}_p(s)\right]d(s)}{1 + \left[G_p(s) - \tilde{G}_p(s)\right]G_c(s)} \quad (20)$$

From this closed loop expression, we can see that if $G_p(s) = \tilde{G}_p(s)^{-1}$ and if $G_p(s) = \tilde{G}_p(s)$, then perfect set point tracking and disturbance rejection is achieved. Notice that theoretically even if $G_p(s) \neq \tilde{G}_p(s)$, perfect disturbance rejection can still be realized provided $G_p(s) \neq \tilde{G}_p(s)^{-1}$.

Additionally, to improve robustness, the effects of process model mismatch should be minimized.

Since discrepancies between process and model behavior usually occur at the high frequency end of the system's frequency response, a low-pass filter $G_f(s)$ is usually added to attenuate the effects of process model mismatch. Thus, the internal model controller is usually designed as the inverse of the process model inseries with a low-pass filter, $G_{IMC}(s) = G_c(s)G_f(s)$ the order of the filter is usually chosen such that $G_c(s)G_f(s)$ is proper.

The resulting closed loop then becomes

$$Y(s) = \frac{G_{IMC}(s)G_p(s)R(s) + \left[1 - G_{IMC}(s)\tilde{G}_p(s)\right]d(s)}{1 + \left[G_p(s) - \tilde{G}_p(s)\right]G_{IMC}(s)} \quad (21)$$

Designing an internal model controller is relatively easy. Given a model of the process $\tilde{G}_p(s)$, first factor $\tilde{G}_p(s)$ intro invertible and non-invertible components.

$$\tilde{G}_p(s) = \tilde{G}_p^+(s)\tilde{G}_p^-(s) \quad (22)$$

The non-invertible component $\tilde{G}_p^-(s)$, contains terms which if inverted, will lead to instability and reliability problem, terms containing positive zero and time-delays.

Next, set $G_p(s) = \tilde{G}_p^+(s)^{-1}$ and then $G_{IMC}(s) = G_c(s)G_f(s)$, where $G_f(s)$ is a low pass function of appropriate order [8], [9],.

10. Determination Controller PI of current i_{dq} based on IMC

The model of system which connected the current i_{dq} and the voltage v_{dq} is of first order of the form:

$$\frac{I_{dq}(S)}{V_{dq}(S)} = \frac{k_{dq}}{\tau_{dq}S+1}$$

Whit

$$\begin{cases} k_{dq} = \frac{1}{R} \\ \tau_{dq} = \frac{L}{R} \end{cases} \quad (23)$$

The controller $\tilde{G}_p(s)$ is the reverse of the transfer function $\frac{I_{dq}(S)}{V_{dq}(S)}$:

$$\tilde{G}_p(s) = \frac{\tau_{dq}+1}{k_{dq}} \quad (24)$$

One will increase the controller $\tilde{G}_p(s)$ relation (24) by a filter f(s) of order one which returns controller IMC $\tilde{G}_p(s)$ suitable [10]:

$$C(s) = \frac{G_c(S)}{1-\tilde{G}_p(S)G_c(S)} \quad (25)$$

$$C(s) = \frac{\tilde{G}_c(S)f(s)}{1-\tilde{G}_p(S)\tilde{G}_c(S)f(s)} = \frac{1}{k_{dq}\lambda_{dq}}\left(\frac{\tau_{dq}S+1}{S}\right) \quad (26)$$

The comparing of equation (26) by the transfer function of PI:

$$C(s) = k_{p_{dq}}\left(\frac{k_{i_{dq}}S+1}{k_{i_{dq}}S}\right)$$

The parameters of the PI, $k_{p_{dq}}$ and $k_{i_{dq}}$ as result:

$$\begin{cases} k_{p_{dq}} = \frac{\tau_{dq}}{k_{dq}\lambda_{dq}} = \frac{L}{\lambda_{dq}} \\ k_{i_{dq}} = \tau_{dq} = \frac{L}{R} \end{cases} \quad (27)$$

11. Determination Controller PI of Active and Reactive Power based on IMC

The open loop transfer's functions of active and reactive power are given as:

$$\begin{cases} \frac{P_{ac}(S)}{I_d(S)} = +\frac{3}{2}\frac{V_d}{(2T_aS+1)} \\ \frac{Q_{ac}(S)}{I_q(S)} = -\frac{3}{2}\frac{V_d}{(2T_aS+1)} \end{cases} \quad (28)$$

The controller $\tilde{G}_{p_p}(S)$ and $\tilde{G}_{p_Q}(S)$ are the reverse of the open loop transfer function of active and reactive power respectively:

$$\begin{cases} \tilde{G}_{p_p}(S) = +\frac{2}{3V_d}(2T_aS+1) \\ \tilde{G}_{p_Q}(S) = -\frac{2}{3V_d}(2T_aS+1) \end{cases} \quad (29)$$

The IMCs controllers of active and reactive power are given as:

$$\begin{cases} C_P(S) = +\frac{2}{3V_d\lambda_P}\left(\frac{2T_aS+1}{S}\right) \\ C_Q(S) = -\frac{2}{3V_d\lambda_Q}\left(\frac{2T_aS+1}{S}\right) \end{cases} \quad (30)$$

The comparing of equation (31) by the transfer function of PI:

$$\begin{cases} C_P(S) = k_{p_P}\left(\frac{k_{iP}S+1}{k_{iP}S}\right) \\ C_Q(S) = k_{p_Q}\left(\frac{k_{iQ}S+1}{k_{iQ}S}\right) \end{cases} \quad (31)$$

Thus the parameters k_{p_P}, k_{p_Q}, k_{i_P} and k_{i_Q} as follows

$$\begin{cases} k_{p_P} = \frac{4T_a}{3V_d\lambda_p} \\ k_{i_P} = \frac{2}{3V_d\lambda_P} \end{cases} \quad \textbf{and} \quad \begin{cases} k_{p_Q} = \frac{4T_a}{3V_d\lambda_Q} \\ k_{i_Q} = \frac{2}{3V_d\lambda_Q} \end{cases}$$

12. Simulation Results

After steady state has been reached, a 1.5 pu step is applied to the reference active power at (t=0.2 s) and later a -0.2 pu step is applied to the reference active power at (t=1.0 s). a -0.5 pu step is applied to reference reactive power at (t=0.2s). The dynamic response of the regulators is observed. Stabilizing time is approximately 0.20 s.

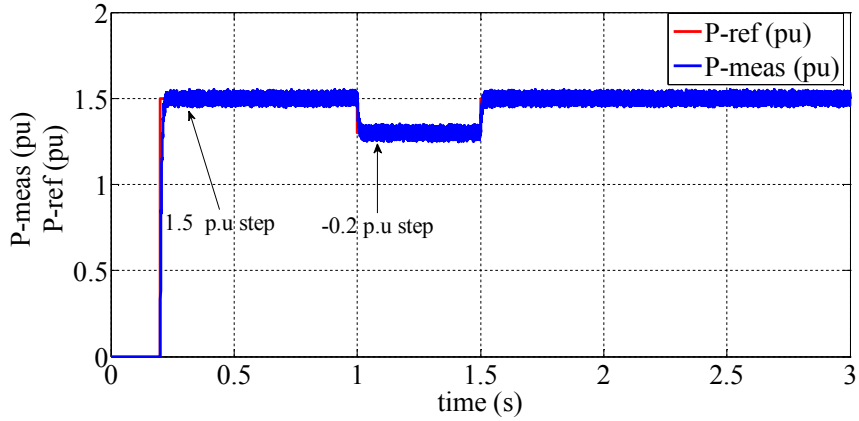

Fig.11. Active Power (pu)

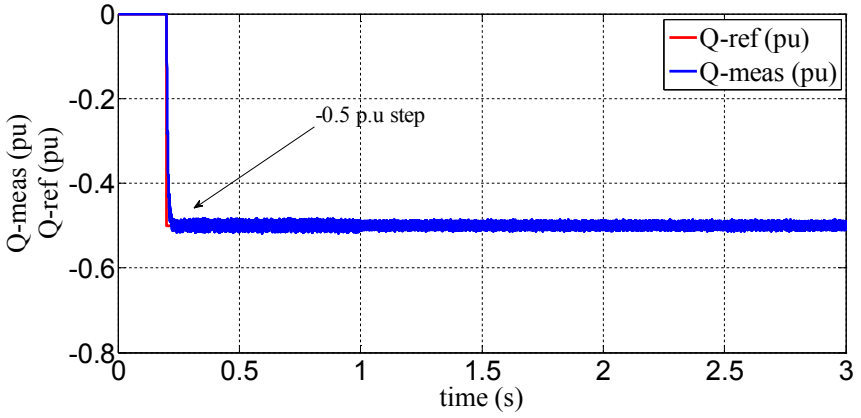

Fig.12. Reactive Power (pu)

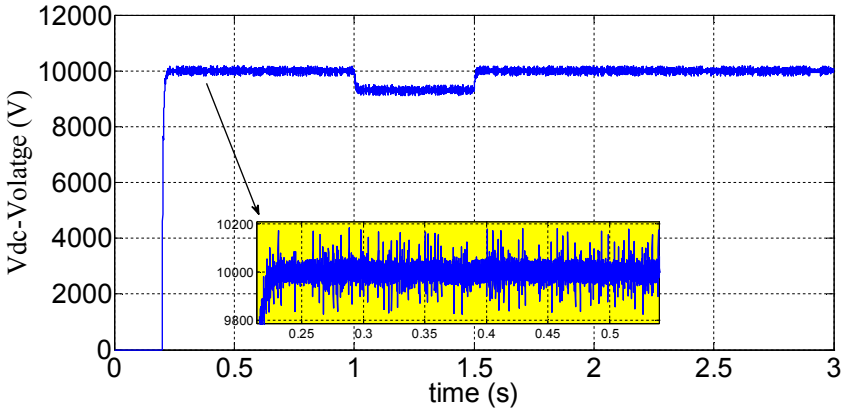

Fig.13 Vdc-Voltage (V)

13.Conclusion

In this work we applied a set of controls on the VSC-HVDC system to connect to the choice of the best controller capable of making this system more capable of working and stability and withstand the disturbances of the devices and external conditions, and the results of comparison between the controls placed on the system are respectively, The control IMC is the best control through the response time; stability ; elimination of disturbances and more performance.the controlled by IMC control of the response time by a low pass filter, this control also has the advantages of relying on the internal mathematical model of the system, which makes it perfect control . The Control by PI is a control that does not make the system more suitable when changing its internal properties and external disturbances. The proposed controls comparisons are a reliable solution to this type of control problem that appears in the smart grid and in connection with renewable energy sources with the power grid.

R E F E R E N C E S

[1]. *Oluwafemi E. Oni; Innocent E. Davidson; Kamati N. I. Mbangula*. A Review of LCC-HVDC and VSC-HVDC Technologies and Applications.*Environment and Electrical Engineering (EEEIC), 2016 IEEE 16th International Conference on.IEEE, 2016.*

[2]. *K.R. Padiyar; Nagesh Prabhu*. Modelling, Control design and Analysis of VSC based HVDC Transmission Systems" 2004 International Conference on Power System Technology.POWERCON 2004 Singapore, 21-24 November 2004.

[3]. *A. Bayo-Salas, J. Beerten, J. Rimez, and D. van Hertem*, .Impedance-based stability assessment of parallel VSC-HVDC grid connections. in 11th IET International Conference on AC and DC Transmission (ACDC 2015), Feb. 2015.

[4]. *L. Wang, M. S. N. Thi,* Comparative stability analysis of offshore wind and marine current farms feeding into a power grid using HVDC links and HVAC line, IEEE Trans. Power Delivery, vol. 28, no. 4, pp. 2162-2171, Oct. 2013.

[5]. *N. R. Chaudhuri, B. Chaudhuri, R. Majumder, and A. Yazdani*, Multi-terminal Direct Current Grid: Modelling, Analysis and Control, NJ: John Willey & Sons, inc. 2014.

[6] *W. Wang, A. Beddard, M. Barnes, and O. Marjanovic,* Analysis of active power control for VSC-HVDC, IEEE Trans. Power Delivery, vol. 29, no. 4, pp. 1978-1988, Aug. 2014.

[7] *Y. Song, C. Breitholtz*, .Nyquist stability analysis of an AC-grid connected VSC-HVDC system using a distributed parameters DC-cable model, IEEE Trans. Power Delivery, vol. 31, no. 2, pp. 898-907, Apr. 2016.

[8] *L. Zhang, L. Harnefors, H.P. Nee,* Interconnection of Two Very Weak AC Systems by VSC-HVDC Links Using Power-Synchronization Control, IEEE Trans. Power Systems, vol. 26, No. 1, February 2011.

[9] *Alisa Manoloiu, Mircea Eremia*. Aspects on control of a vsc-hvdctransmissionlink. U.P.B. Sci. Bull., Series C, Vol. 78, Iss. 4, 2016

[10] *T Allaoui, Ma Denai, M Bouhamida, C Belfedal,*Robust control of unified power flowcontroller (UPFC)IU-Journal of Electrical & Electronics Engineering?vol. 7, no. 1, pp. 331- 343, 2007.